A coupled finite element - discrete element approach for a fine estimation of the crack pattern in concrete subjected to THM loading

A. Delaplace[1], B. Bary[2], G. Kwimang[1,2]
[1] *LMT (ENS Cachan/CNRS/UPMC/PRES UniverSud Paris)*
61, avenue du Président Wilson, 94235 Cachan, France
[2] *CEA Saclay, DEN/DPC/SCCME/LECBA, Saclay, France*

1 Introduction

Durability of civil engineering structures under thermo-hydro-mechanical (or THM) loading is still a high challenge, especially for nuclear installations. A THM model has been developed for this purpose, allowing reproducing the behavior of concrete subjected to moderate heating. In a first approach, the mechanical parameters, Biot coefficient and permeability evolutions are estimated from an isotropic microcracks distribution. Nevertheless, these properties highly depend on the crack pattern. A more reliable description of the latter can be obtained by using a discrete element model which is pertinent to describe crack pattern. Cracking in the material has multiple influences in the THM behaviour of the material. We propose in this study to focus on the impact of the cracking on the permeability. In a first part, the outline of the THM model is proposed, with a particular attention to the permeability parameters. In a second part, the discrete model used to describe cracking is presented. Finally, the third part illustrates the proposed procedure to link the crack pattern computed with discrete model to the macroscopic permeability evolution of the THM model.

2 Thermo-hydro-mechanical model

The mechanical behaviour of the THM model proposed here is based on the Biot formulation (see for example [1] for a review). For a strain tensor $\boldsymbol{\varepsilon}$, the stress $\boldsymbol{\sigma}$ is gained as [2]:

$$\boldsymbol{\sigma} = 2\mu\boldsymbol{\varepsilon}^D + 3k\ \mathrm{tr}(\boldsymbol{\varepsilon})\mathbf{I} - b\mathbf{I}p_l - 3\alpha k(T - T_0)\mathbf{I} \tag{1}$$

where superscript ^{D} refers to the deviatoric part of the tensor and $\mathbf{I}$ is the second order identity tensor. Material parameters are the shear and bulk moduli, respectively μ and k, the Biot coefficient b and the coefficient of thermal expansion α. T_0 and T are respectively the initial and the current temperatures. p_l is the liquid phase pressure, assumed here to be equal to the inverse of the capillary pressure. This pressure is obtained from the governing equation of the liquid in the material, computed from the mass conservation equation:

$$(S_v\rho_v + S_l\rho_l)\frac{\partial\phi}{\partial t} + \phi\left(\rho_l\frac{\partial S_l}{\partial t} + \rho_v\frac{\partial S_v}{\partial t} + S_l\frac{\partial\rho_l}{\partial t} + \S_v\frac{\partial\rho_v}{\partial t}\right) + \\ \nabla(\mathbf{w}_l + \mathbf{w}_v) + \phi(S_v\rho_v + S_l\rho_l)\frac{\partial \mathrm{tr}(\boldsymbol{\varepsilon})}{\partial t} + \frac{\partial m_s}{\partial t} = 0 \quad (2)$$

In this equation, subscripts $_l$ and $_v$ designate the phases of liquid, respectively in water and in vapour. m_i is the mass per unit material volume of liquid in phase i, m_s is the mass of solid skeleton. ρ_i is the density of liquid in phase i. S_l is the saturation degree, $S_v = 1 - S_l$, ϕ is the total porosity. The mass flux $\mathbf{w}_i$ of liquid in phase i depends on the material permeability. A first development of the model considers an isotropic distribution of the permeability [2]. This simplification is acceptable under particular loading condition like hydrostatic loading. On the other hand, this assumption is too strong if cracking is oriented by the loading, for instance cracks perpendicular to the loading direction in a simple tension test. In the latter, we consider a more general case where the permeability is expressed as a tensor.

The permeability tensor of the cracked porous medium results from the contribution of the initial connected porosity and the one of the cracks. In this study we make the distinction between diffuse microcracks and localized macrocrack, since the latter case constitutes a privileged path for macroscopic hydrous transfers whereas the former one represents a set of non-connected microcracks whose influence on the overall transfer properties is of much lesser importance and may be neglected in first approximation. The permeability tensor is written as $\mathbf{k} = \mathbf{k}_e + \mathbf{k}_c$ with $\mathbf{k}_e$ and $\mathbf{k}_c$ the permeability tensors of the intact material and of the cracks, respectively, which depend on the saturation state. We further assume that the macrocracks are only filled with gaseous phase, as a consequence of the thermo-hydrous loading conditions considered here (*i.e.* thermal loading inducing dessiccation of the material). The fluxes are then expressed by making use of the Darcy's law as:

$$\mathbf{w}_i = -\rho_i\frac{\mathbf{k}}{\eta_i}k_{ri}\nabla p_i \quad (3)$$

k_{ri} and η_i are the relative permeability and the dynamic viscosity of the phase i, respectively ($i \in \{l, v\}$). Considering in each finite element only average macrocracks with mean orientation and aperture, and expressing the gas flow occurring in the cracks in the form of a Poiseuille flow [3], we get:

$$\mathbf{k}_c = \sum_i \frac{\lambda_i}{12}e_i^2(\mathbf{I} - \mathbf{n}_i \otimes \mathbf{n}_i) \quad (4)$$

where $\mathbf{n}_i$ and e_i are the orientation and aperture of the macrocrack i, respectively; λ_i is a parameter accounting for the effects of rugosity and tortuosity.

3 Discrete model

3.1 Model basis

The discrete model used in this study is based on an assembly of particles, generated from a Voronoi tesselation of randomly distributed points [4]. Material cohesion is obtained by introducing elastic beams linking the nuclei of two neighbouring particles [5]. A perfect elastic brittle behaviour with a random threshold value is assigned to each beam. If the strain in a beam exceeds the threshold, the beam breaks irreversibly (figure 1). Although this discrete model is very simple, complex behaviour is obtained, like the non-symmetric behaviour of concrete in tension and compression [6, 7, 8, 9, 10]. The 3D formulation of the model, not considered in this paper, is strictly similar [11].

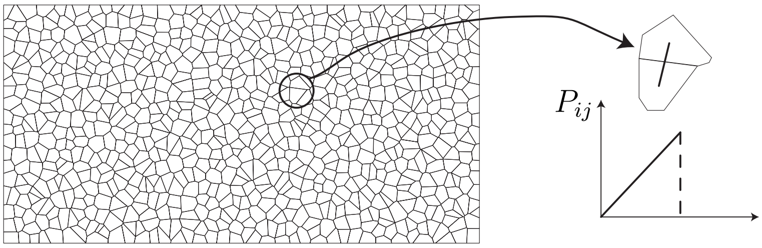

Figure 1: Description of the discrete model.

3.2 Crack description

Discrete model allows a realistic description of cracking, due to its natural description of the material by an assembly of particles which can break under certain loading. In particular, crack roughness is well rendered with this approach [12, 13, 14]. This is a key point when considering the present problem, *i.e.* permeability evolution through a breaking sample. In the model, a crack is created when a link breaks (irreversibly) between two particles i and j. Crack path is linked to the common segment of the two particles: crack length ℓ_{ij} is the segment length, crack direction is given by the orientation of the segment (figure 2). Crack opening e_{ij} is evaluated by computing the difference of the displacements $\mathbf{u}_i$ and $\mathbf{u}_j$ of the two particles projected to the normal of the crack: $e_{ij} = \langle(\mathbf{u}_j - \mathbf{u}_i).\mathbf{n_{ij}}\rangle$ using the notation $\langle x\rangle = \max(x, 0)$ for the positive part of a scalar.

Crack description obtained at the microscale, *i.e.* the discrete element model scale, is transmitted at the macroscale, *i.e.* the THM model scale. For each macro-element h, equation (4) is applied for all cracks lying in the considered element. We consider here in a first approximation that λ_i equals one. Finally, a permeability tensor is evaluated for each macro-element.

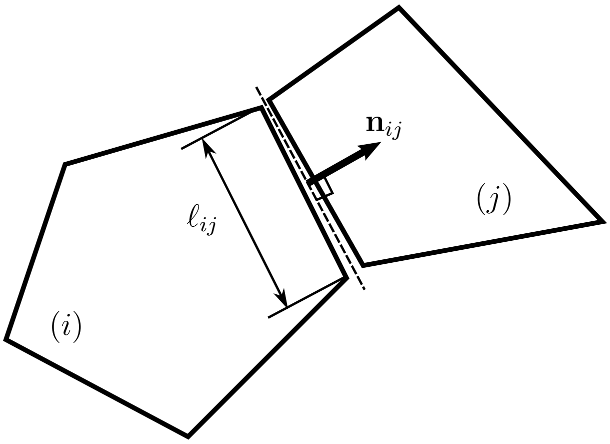

Figure 2: Description of a crack between two particles.

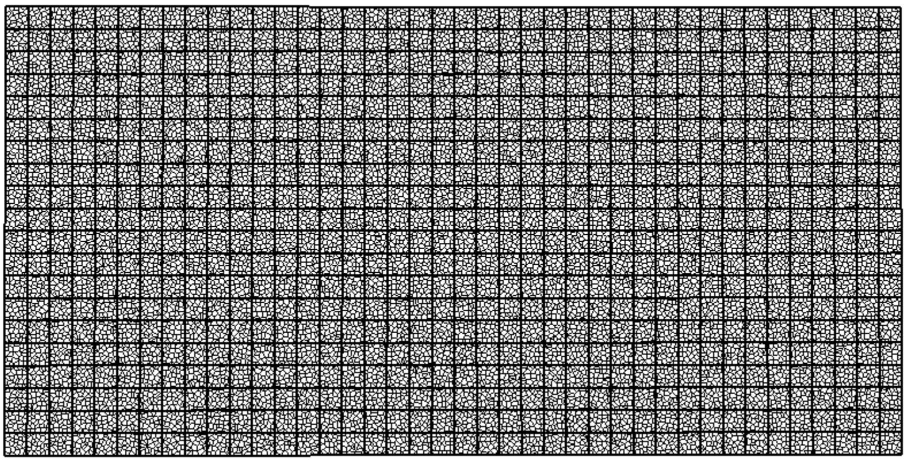

Figure 3: Micro- and macro- scale meshes.

4 Crack analysis on a simple tension test

We propose here to illustrate the procedure on a simple tension test. The geometry of the beam and the loading conditions are shown on figure 4-left. We use a 200x100-particle mesh. Peak load is obtained after the breaking of 273 fibers, the global failure is obtained after the breaking of 684 fibers. The global response force-displacement is plotted on figure 4-right.

The global failure occurs after the propagation of a macro-crack through the sample, perpendicular to the loading direction. Two crack patterns are representing on figure 5. The first one is obtained just before the peak load (before strain localisation), as the second one is obtained just before failure. One can see that before the peak load, a network of homogeneously distributed cracks is visible. The homogenisation procedure presented above is used to estimate the permeability parameters for each element of the FE mesh shown

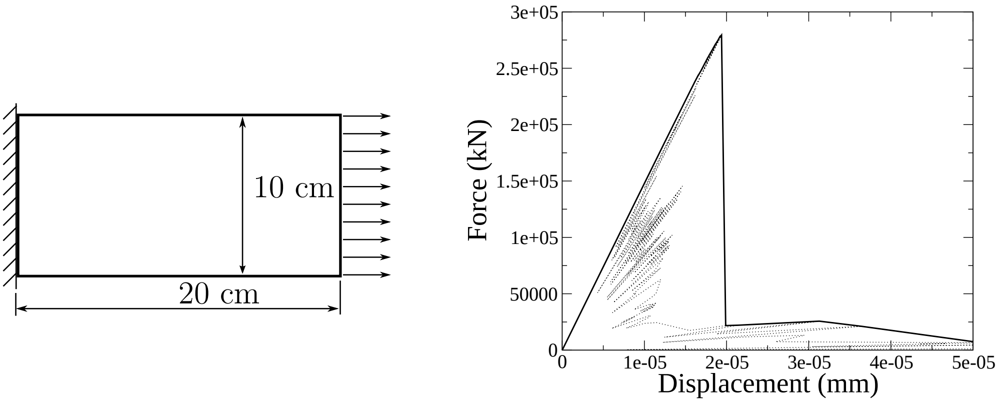

Figure 4: Geometry and loading conditions of the tension test (left) and force vs. displacement response (right).

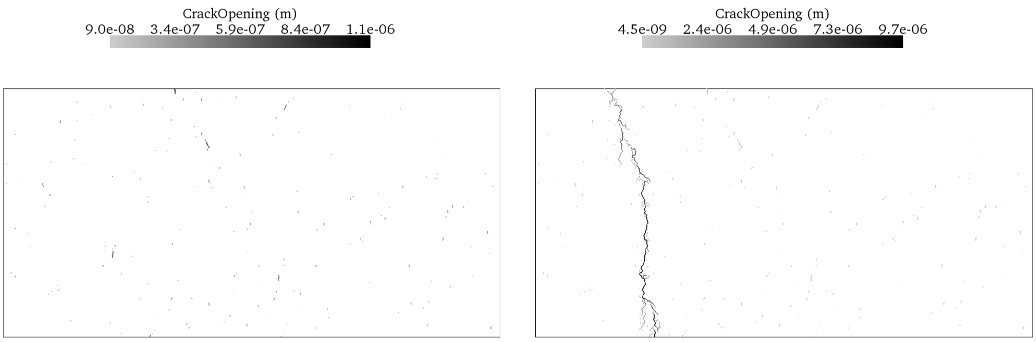

Figure 5: Crack patterns before peak load (left) and before complete failure (right).

in figure 3. The coefficient of the permeability tensor are plotted on figure 6. The first line corresponds to the peak load as the second one is obtained just before failure. As expected, the permeability evolves from an homogeneous state before localisation, and tends to a single oriented line at failure. Another remark is that permeability may locally decrease with the closure of the unloaded microcracks.

The example shows clearly the advantage to consider a tensor for the permeability variable rather than a simple scalar. A complete THM example using such permeability map is under progress and will be presented during the conference.

5 Conclusion

We propose in this study a two-scale approach to take into account a fine estimation of the crack-induced permeability, with for objective the study of the thermo-hydro-mechanical behaviour of concrete under moderate temperatures. In fact, crack density, crack opening and crack orientation have a strong influence on the transport properties and should be incorporated in the model at the macroscopic scale. To obtain such fine description of cracking, we use a discrete model, which describe naturally cracking in brittle material. Homogenisation is performed for each macro-element in the THM model, using the approximation of a Poiseuille flow.

References

[1] O. Coussy. *Poromechanics.* John Wiley & Sons, New York, 2004.

[2] B. Bary, G. Ranc, S. Durand, and O. Carpentier. A coupled thermo-hydro-mechanical-damage model for concrete subjected to moderate temperatures. *International journal of heat and mass transfer*, 51:2847–2862, 2008.

[3] L. Dormieux and D. Kondo. Micromechanical approach to the coupling between permeability and damage. *C. R. Mécanique*, 332:135–140, 2004.

[4] C. Moukarzel and H. J. Herrmann. A vectorizable random lattice. *J. Stat. Phys.*, 68:911–923, 1992.

[5] J. G. M. Van Mier, M. R. A. Van Vliet, and T. K. Wang. Fracture mechanisms in particle composites: statistical aspects in lattice type analysis. *Mech. Mater*, 34:705–724, 2002.

[6] P. A. Cundall and O. D. L. Strack. A discrete numerical model for granular assemblies. *Géotechnique*, 29:47–65, 1979.

[7] F. Kun and H.J. Herrmann. A study of fragmentation processes using a discrete element method. *Comp. Meth. Appl. Mech. Eng.*, 7:3–18, 1996.

[8] F. Camborde, C. Mariotti, and F.V. Donzé. Numerical study of rock and concrete behaviour by discrete element modelling. *Computers and Geotechnics*, 27:225–247, 2000.

[9] F. Alonso-Marroquin, S. Luding, H.J. Herrmann, and I. Vardoulakis. Role of anisotropy in the elastoplastic response of a polygonal packing. *Physical Review E*, 71:051304, 2005.

[10] A. Delaplace and A. Ibrahimbegovic. Performance of time-stepping schemes for discrete models in fracture dynamic analysis. *International Journal for Numerical Methods in Engineering*, 65:1527–1544, 2006.

[11] A. Delaplace and R. Desmorat. Discrete 3d model as complimentary numerical testing for anisotropic damage. *International Journal of Fracture*, 148:115–128, 2007.

[12] E. Bouchaud. Scaling properties of cracks. *J. Phys. Condens. Matter*, 9:4319–4344, 1997.

[13] A. Delaplace. Fine description of fracture by using discrete particle model. In *ICF 11 - 11th International Conference on Fracture*, 2005.

[14] S. Santucci, K. J. Måløy, A. Delaplace, J. Mathiesen, A. Hansen, J.O.H. Bakke, J. Schmittbuhl, L. Vanel, and P. Ray. Statistics of fracture surfaces. *Physical review E*, 75:16104, 2007.

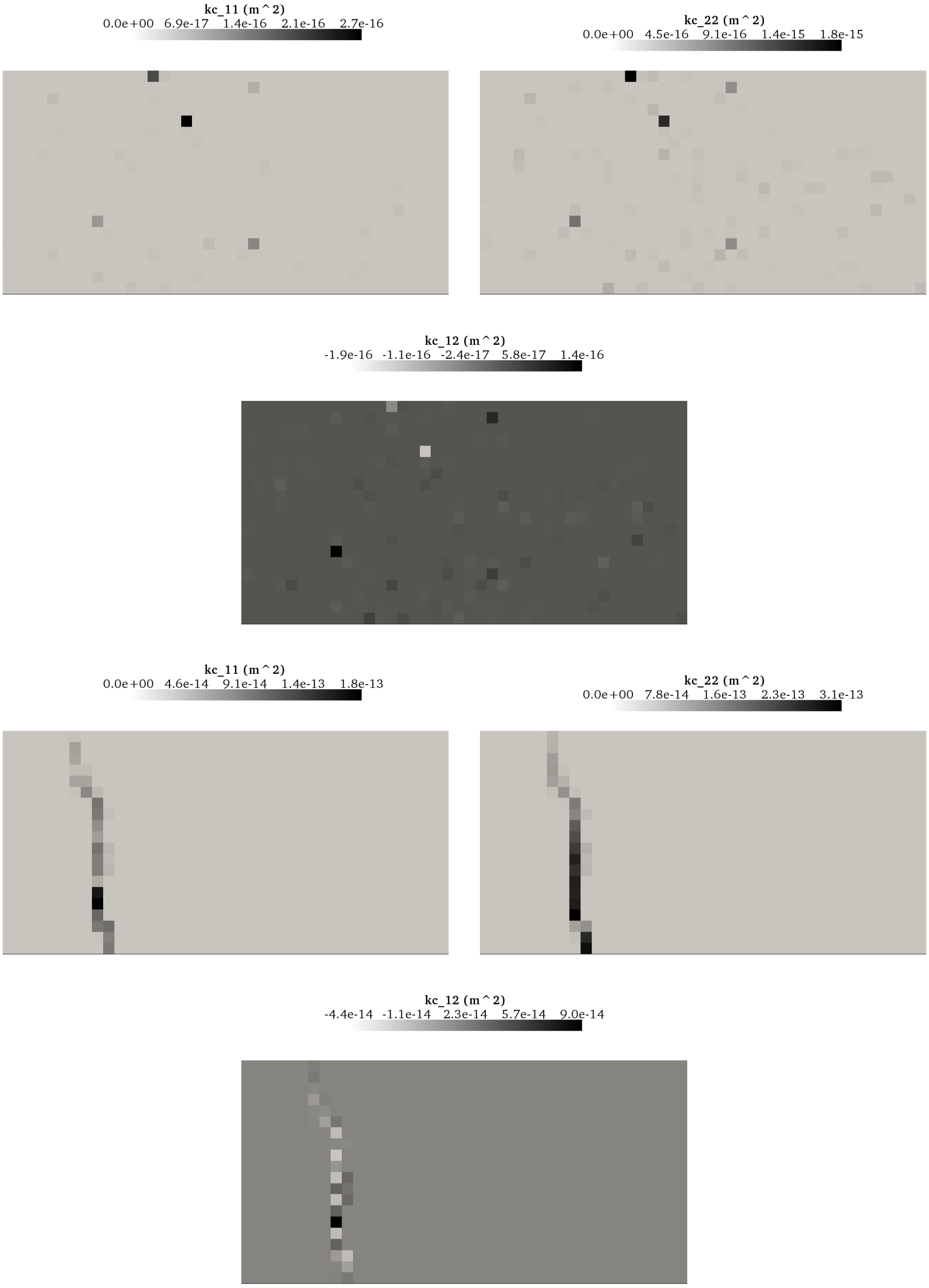

Figure 6: Permeability tensor maps computed from the discrete model crack pattern, before the peak load (top) and at the end of the loading (bottom).